Supporting Information:

Large-Conductance Transmembrane Porin Made from DNA Origami

Kerstin Göpfrich, Chen-Yu Li, Maria Ricci, Satya Prathyusha Bhamidimarri, Jejoong Yoo, Bertalan Gyenes, Alexander Ohmann, Mathias Winterhalter, Aleksei Aksimentiev, Ulrich F. Keyser

Contents

1. Layout and DNA sequences of the DNA origami porin

1.1 Pathways of DNA strands

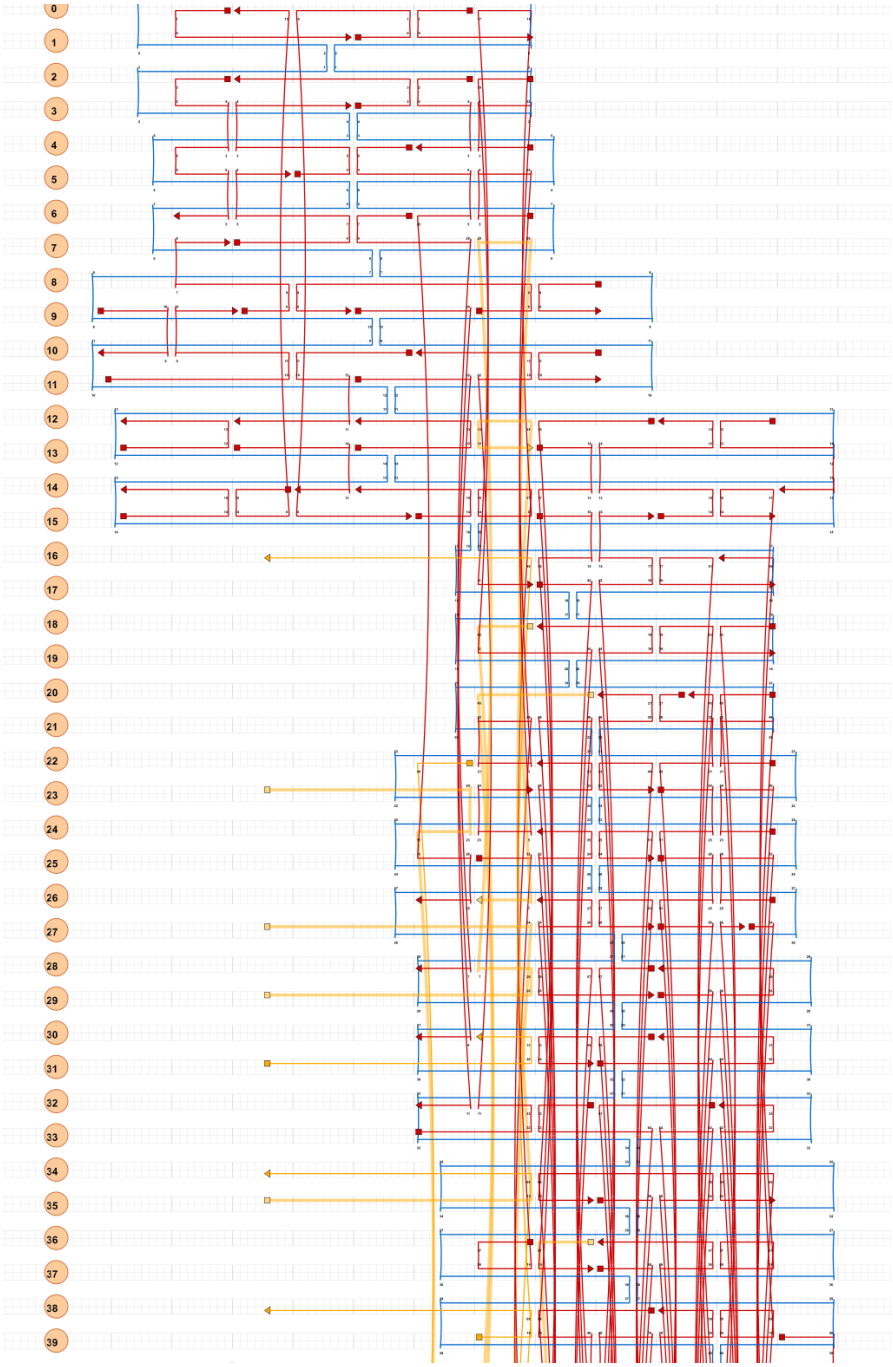

Figure S1. Pathways of the M13mp18 scaffold (blue) and the 179 ssDNA staples (red) of the funnel-shaped DNA origami. SsDNA overhangs for hybridization with complementary cholesterol-tagged oligos are shown in orange (1).

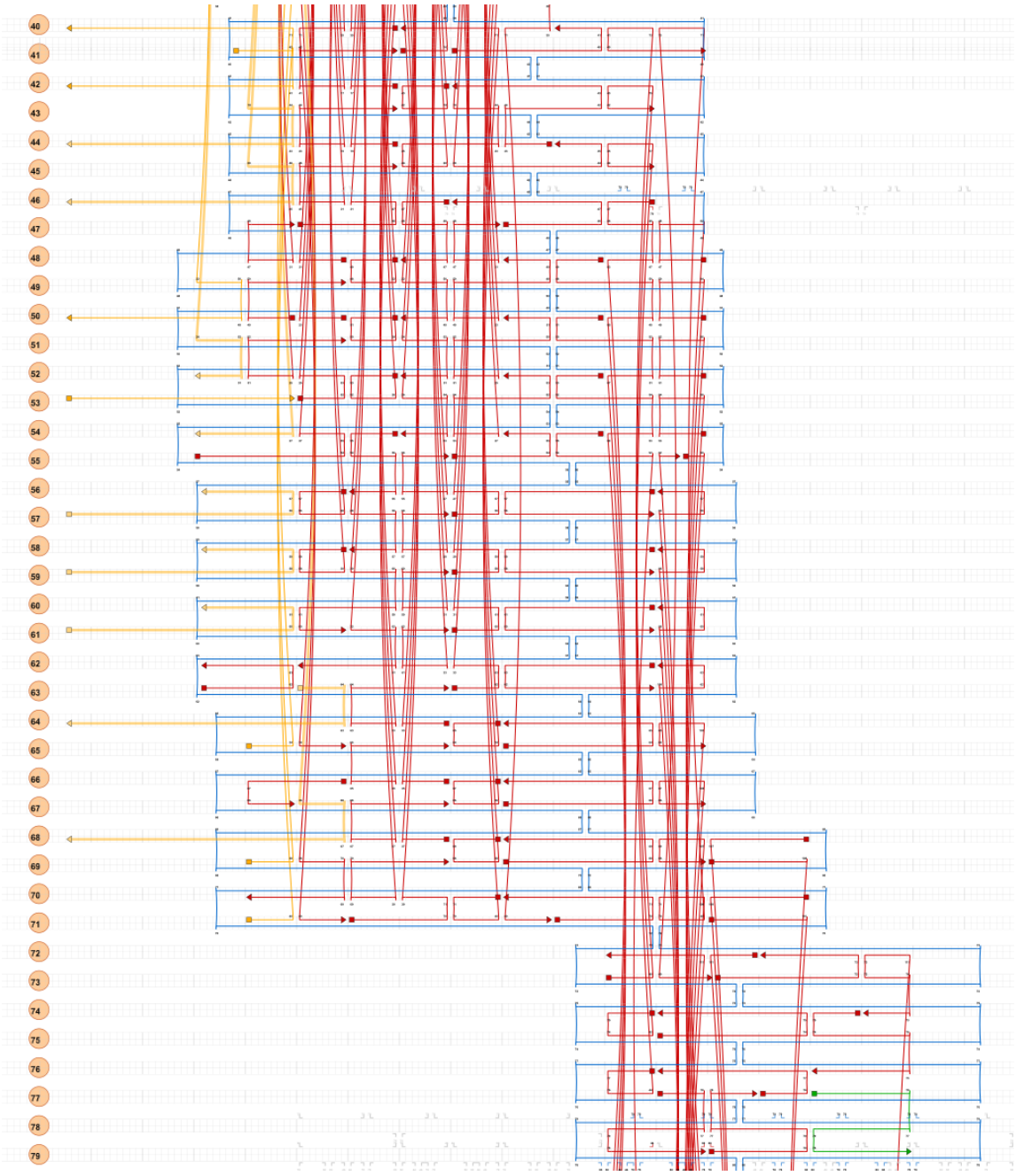

Figure S2. Continued: Pathways of the M13mp18 scaffold (blue) and the 179 ssDNA staples (red) of the funnel-shaped DNA origami. SsDNA overhangs for hybridization with complementary cholesterol-tagged oligos are shown in orange, oligos with optional Cy3-tags are shown in green (2).

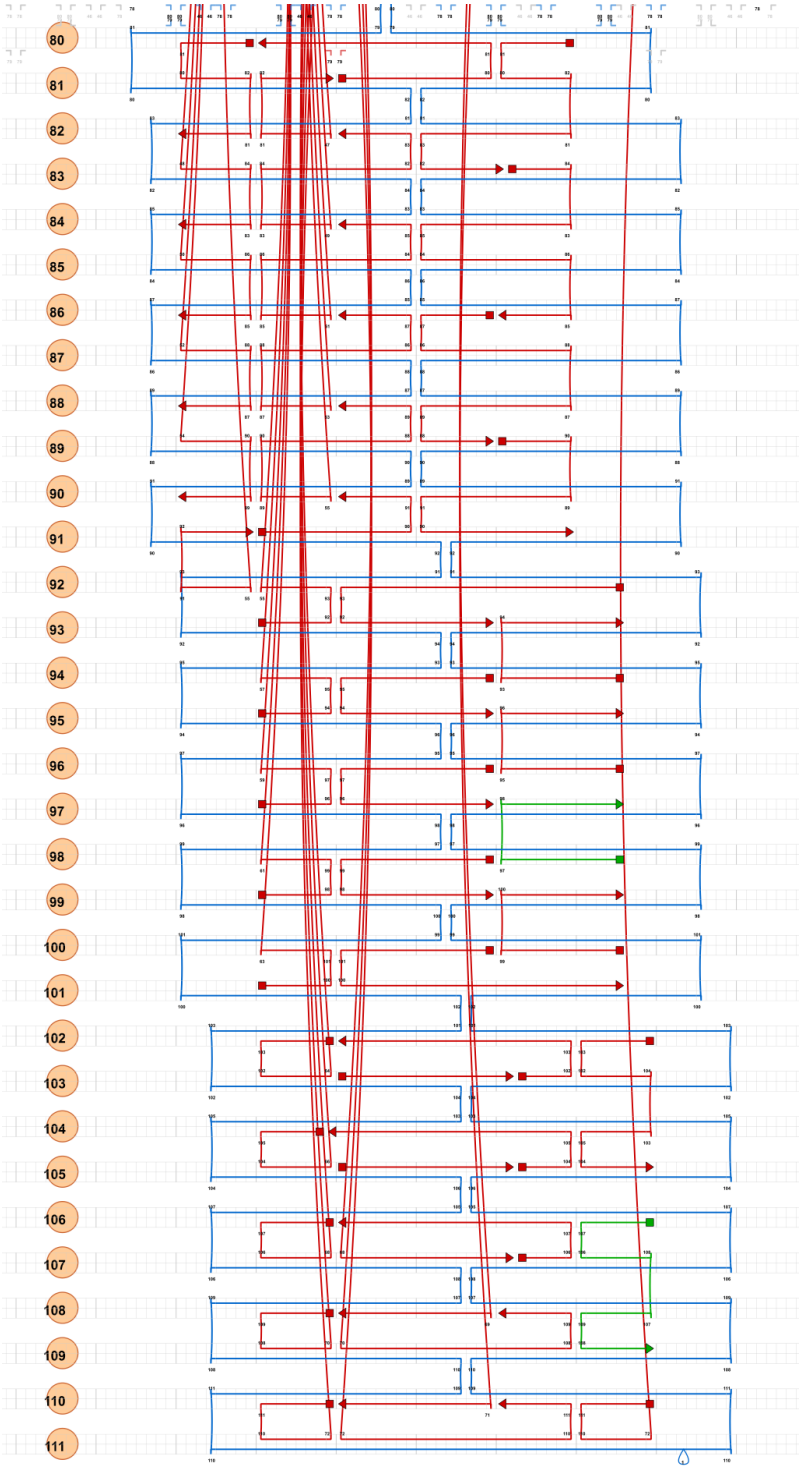

Figure S3. Continued: Pathways of the M13mp18 scaffold (blue) and the 179 ssDNA staples (red) of the funnel-shaped DNA origami. SsDNA overhangs for hybridization with complementary cholesterol-tagged oligos are shown in orange, oligos with optional Cy3-tags are shown in green (3).

4.2 Positioning of cholesterol anchors

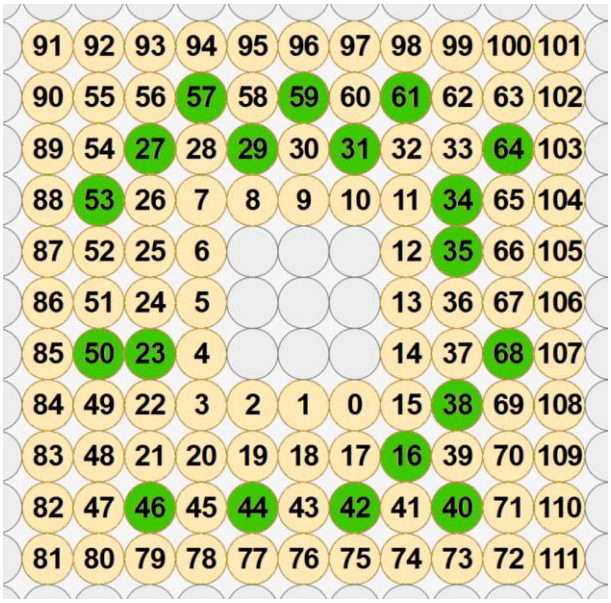

Figure S4. Positions of 19 ssDNA overhangs for hybridization with cholesterol-tagged oligos (green). Every circle corresponds to one DNA duplex, looking at the funnel-shaped DNA origami along the pore axis.

1.3 DNA sequences

Table S1. DNA sequences of the funnel-shaped DNA origami (1).

Name	Sequence
Core1	ATAATTACTAAATAAGCCGACCGTCCGGCACCTTCGCCAT
Core2	AATTAGCAAGAACGGGTCGCAAATCCCAATTC
Core3	AGTATCGGCCGCCTGCAAAAATCTAAAATGGGCGCATCGT
Core4	GCCCCAGTCCTGTTTCAATAACGCAGTACCT
Core5	TGGCCTTCCTGTATGAGGATTTAGCGTTATTAATTTTTTAACCAATAG
Core6	TGAAACCATCACCAGTAGCACCATATTAGAGCAGCGTAACGTAAATGA
Core7	AGCTACAAAAGATTAGTAAAAACCTGCCAGAG
Core8	AAAGTGTAACACAACAGAATCCTTCGATAGCT
Core9	TTACCAACCAGTTACAGGCTCATTTTACCTTATGCGATTTAAGCTGCT
Core10	TCAGTGTCAAATTACAGTAGGGCTCATGTAATTTAAAAAGAATACACT
Core12	AGACAGTCAAATCATATACAGTAAGATTCGCCTGATTTATTTCAACGC
Core13	CACACGACATTTACATTGGCAGATCCGCCTACATTTTGAC
Core15	GCCGCCACGCCACCCTCCACCACCGCCGCCAGTGGCCTTG
Core16	GTTTACCAAAAAGGAAGTTTTGTCTGTAGCAT
Core17	CTCAGAACACCCCCAGTGCCACTACGAAGGCA
Core18	AGCGTCATACCCTTGAGTAA
Core19	AAGGATAAAAGGCCGGGAAAAATACAACAATAGCCCTTTTAATAGCAA
Core20	CAGGACGTGTAGAAAGGCGTCTTTTTGCACCC
Core21	TGTAGGCATCACCTTGAGTTGAAAGGACGTGGTTCTCATT
Core22	CAGCAAAAGCCGAATTATCACCGTGAATAGAA
Core23	GTTGCAGCAAGCGATGGT
Core24	GAACGCCATTCGCGTCAACGCCAATAATTGAG
Core25	ATTTGGGATACCATTATCCACAGATACAAACT
Core26	TATCGGTTCAGCTTGATACCGCCAAAATTAAGTCAATTCTACTAATAG
Core27	AAAACGCTCATGGAAATAAGCTCGAATTCATTGTTATCCGCAGAA
Core29	GATCTAAATTACGAGGAACAACATTATTACAG
Core30	TAGTAGCAGATACATTTATTAAACACTCATCG
Core31	AGACAGGAACGGTCCTGAGAAGTGTT
Core32	CTTGCCCTCTTTAATCTCCCAATCCCAGAGCC
Core33	GAATGCCAAGCTCGACGTTGTAAAACGAGGCGATTA
Core34	TGGATTATACTTCTGACGTGGACTCCAACGCCCCCGATTTGAGAAAGG
Core35	AAACCGTCATGGCCCATCAGATGAGTTAAAAT
Core37	GGCGGATACCGGAATACATCTTTT
Core38	CCGTCGGAGAACAAACGGCGGATTGGATAGGTCACGTTGG
Core39	TGATATAAGTATAGCAGTGCCGTCGAGAGG
Core42	GTATGTTAATGATTAAGACTCCTTTTACCGAA
Core44	ATATTTAAAGAACCCTAACATTATGACCCTGT
Core45	CTGGAGCAAACAACTACCATATCAACGTCAGATGAACCATCAATATGA

Table S2. DNA sequences of the funnel-shaped DNA origami (2).

Name	Sequence
Core46	CTTAAATCTTTTATCCCAACTAATGTTGAGATTTAGGAATTAAGAACT
Core47	CATCAATATAATCCTGGGAGTCAAAGGGCGAA
Core48	AATCGGCCCCTGTCGTTTTCATTTTTTTAATG
Core49	TGCCCGTATAAACAGTTAATGCCCCTTTAACGGGGTCAGTGATGGCTTTT
Core50	GGAGGTTGAGAGCCGCCACCAGAACAGAGCCACCACCCTC
Core51	AGGTGAATTTCTTAAATATCAGCTACACCACGATTCATATGGTTTACC
Core52	GGGGTAATCATTGAATTCAGGTCT
Core53	AGCAAATGAACAGTGCGCGGTCAGTATTAACACCGAACGAA
Core54	GTTTAGAAGTTTAAAATAGCGAGAGGCTACCACATT
Core55	CATATATTTTAAATGCTAATGTGT
Core56	AGACTCCTCAAGAGAAAAGTATTAAGAGGC
Core58	ACAGCCATTTTTGTTTCATTCAGTCCAAATCA
Core59	GCGACATTCGGAAATTATTCATTAAAGGTAGAATGGAAAGCAGGAGTG
Core60	ACGCTCAGCAGCGAAACTACAAAGAATCATATGTACCCCG
Core61	TTCTTTGATTAGTCTTGCCTGAGTAG
Core62	CATAGCCCCGCGTTTTCATCGGCA
Core63	ATCAAGTTAGCACCGTGTCACCAA
Core64	TGCGAACGATAATGCTATCGTAGGGCGCCCAATAGCAAGC
Core65	GAGTCCAGTCGGGAAAAACGCGCGGGGAGAAT
Core66	AACCGTGCTTGAGGGGCTCCAGCC
Core67	GATGATACGCAGTCTCTGAATTTACAAACAA
Core68	GACTGTAGCCTTATTAGCGTTTGCGGTGTATCACCGTACT
Core69	AAATCTAAGATAAGAGACATGTTTTAAATATGCATATAAC
Core70	GCGACAGAGCCACCCTCAGAGTACACTTAGCCAAGTACAACGGAGATT
Core71	AAATCATATAGGTTGGAGTTGGGTGGGGGATGTGCTGCAACGGTGCGG
Core72	ACGCCAGAGGCGGTTTACCAGTGAGACGGGAGCTAAACAGGAGGC
Core73	GACGAGAAAGCCCAATAGGCTGGCTCATAAGGGAACCGAA
Core74	CGACAATAGGTAAAGTTTAAATTG
Core75	AACGTCAACTTTGAAAGAGGATGTTTAGTATCGCCAACGC
Core76	GAGGAAGGGATAATACATTGCCAGCTTTCATC
Core78	CAGGAGGTACCAGAAGGAATTGCT
Core79	TCGATAGCTGCCTTTAGCGCGCCTCCCTCAGA
Core80	AATAAGCCTAATGAGTTGCCCGCTTTCTGTCC
Core81	AAACGAAAGAGGCGGCAGAGGCATCGACAAAA
Core82	AGGATTAGGATTAGCGCAGTACCA
Core83	AGCGCTGGTAATAAGTCTGCCTATATTATTCTGAAACATG
Core84	TAGAAGGCCGAACCAGAAGCCCGA
Core85	GGGTTACCGAGGAAACAACATATAAAAAACCT

Table S3. DNA sequences of the funnel-shaped DNA origami (3).

Name	Sequence
Core86	AACGGAATATAGCCGACGGGATCG
Core87	TGGGAAGAACAACGCCAGGAACCC
Core88	AAAACAAAATTAATTTGACCATTATTAACATCCAATATACCTGAGCAA
Core89	GAAACAGTACATAAATTGCTGAATAGTAGATTTAGTTACATTTAACAA
Core91	CAATAGAAAGAATAAGTT
Core92	GTGATAAAAATTTCATCTTCTGACCAAATATATGCGCAACGCTATTAC
Core95	GGCCTTGCTGGTACAATATTACCGCC
Core96	AAATTTTTTTTACGAGTCCTTATCATTATAGTTGCGCCGAGTACCAAA
Core97	GCAAGTGTAAAGGAGCAACGTGGCAGAGCTTG
Core98	AATGCTTTAAACAGTTTTTGCAAA
Core99	AACAATGATAAGAAAAGTAAGCAGACCCAAAAGAACTGGCGCAAACGT
Core100	TTACCCTGCAAAAAGAAGTTTCAGATTGCGAATAAAGATA
Core101	CCGGAAACAATCAGTAATGTACCGGGATAGCAACACCAGAAGTAATCT
Core102	TTATCTAAAATATCTTCAGTTGGCAAATCAACCTGAACCTCAAATATC
Core103	AGAAAATACATACATATAACCGAT
Core104	AAGACTTCGACCATAAGGAG
Core105	CATTTTAAAAGTTTGAGTAACATGAATTATCATCATATT
Core106	ATAAATCCTCATTAAAAGGCAGGTCAGACGATCATTGACA
Core107	CGAACAACTTAAGAGGACCGGAAG
Core109	TGCTTTAATCAGAGCGGGCAACAGCTGATT
Core110	AACTTTTTCTAAATTTAAGCGCCAGCTTCTGGTGCCGGAACCTCAGGA
Core111	TGTGTGAAGTAATCATTAGT
Core112	TGCGGATGCTTCAAAGTTATCCGGACGCGAGGCGTTTTAG
Core113	TGACAAGAACCGGATAAGGCGCATCAAATAAGATAGCAGC
Core114	TCACCCGCCTGATAAAATTCAAAAGGGTGAGA
Core115	AATAATAAACCCACAAGGCTACAGAAGTTTCCCCCAAAAA
Core116	CCACCGAGTAAAAATCACGCAAATTA
Core117	GAAAAAACGATTATTATTTAATTGTGAAATACCAGT
Core118	AGGCAAAGAATACTTTGCTGTCTTCATGTAGA
Core120	TTGCAGGGCGCTTTTGACAAAGTTTTAAGCCCTTTTCGGTCCGCCACC
Core121	TAGATTAAGACGCAAAACGAGAATAAATATCGCGTTAATTTTCCCTTA
Core122	AAAATCTAGATGGTTTAATTTCAA
Core123	CCACCAGATCGCCATTAAAAATACTATTAGTCTTTAATGCAATATTT
Core125	CAGGAAGATTGTATAAGTAAAACTAGGACTAAAATGCAGA
Core126	TACAGACCTTCATTACGAATAAGG
Core127	TAATTTGCGCTAACGAATTCATCAGCAGATAC
Core128	AAGCGCATCGCCTGATGAAATCCGCGACCTGCCTGACCAAAAAT
Core129	GTAACCGGGCGCGTACTGTCCACGCTGGTTT
Core130	ACGTAACATAAGGCGTTAGAAAAGCCCAGATGAACGGTG

Table S4. DNA sequences of the funnel-shaped DNA origami (4).

Name	Sequence
Core131	TTCTTTTCGCGTATTGAAGAAGATACATCAAG
Core132	GACTTGCGATCAAAAACCCCCTCA
Core133	AAAACACTTGTATCATTAGACGGGTAACATAAAAACAGGG
Core134	GGGCGCGAGCTGAAAAGCTATATTTTCATT
Core136	AGACTACCCAGTGAGAAGAGTCAAGGTCATAGTCGACTCT
Core137	AATCGGAAAGTTTTTTAAGGAGCGTATCATTTAAATCCTT
Core138	ATATCCTCACAATTCCAAGCCTGGGGTCATCA
Core139	TACTGCGGAATCGTCATAAATATTAGTAAAATAAACAACTGTCTTTCC
Core140	AACATTAAGTAACAACAGTATAAAATATGCGT
Core141	ATAACGCCGACGACGATTGCTATTTTCCTCCC
Core142	TAACTATAAAAGAACGGCCTCTTCTGTTGGGAAGGGCGATACCAGGCA
Core143	AAAGCGAGCGGTCACGCAAATCGGCAAAAT
Core144	TGGAACAATTAAAGAAATAATGGATGGCAATTAGAGAATAAAATCAGCT
Core145	TATTCAACCTGAGAGTGTTCAGCTCCAGACGATTGAGCGC
Core146	CTCGTTAGGACGAGCACCGCTACAACCACACC
Core147	TCATGAGGAGGCTTTGAGCATGTCGCTATCAGGTCATTGC
Core148	AGAGGATCCCCGGGTACGGCCAGT
Core149	GCGCTCACGAGCTAACGAGTGAATCTGTAAAT
Core150	TACCAAAGACAAAAGGATCTCCAA
Core151	TGCACGTAAAACAGAAAAGTGTTGTTCCAGTT
Core152	TAACGTTTTTATTTTCGTAGCTCAGTCATTTT
Core153	CATCTTTGACCCTGAAGAGAGATAGAGCAAGA
Core154	CGGTAATCGCAAATATAATTCTGTAGACTTTT
Core155	CATAATCAAACCAGAGCCACCACCGGAACTCA
Core156	AAATTGCGTAGATTTTAGATAGGGTTGAGGGAAG
Core157	TCCATGTTAGAGAGAAAGAATTAACTGAACCG
Core158	GATGGTGGTTCCGTGCGC
Core159	AAATATTGACAACCGATT
Core160	TTGAAATAAATAAACAAGATCGCAACGACGAC
Core161	CCCTTATAATAGCCCGCAGGTTTAAAATTATT
Core163	TAAACGTTAATATTTTAGGGTTAGAACGAGAATCGATGAA
Core164	CTGATGCATTTTTAACCTCCGGCTGGTCTGAGCCCAGTCATGCATGCC
Core165	TGCCCGAAAAGTATTAGACTTTACATTAGAGCCGTCAATA
Core166	CAAACTCCCTCCTTTTTTTTTTCAGGAGCCTT
Core167	TGCGGGAGAAGCCTTGCTTTGAATTTCATTTCAATAATCATACAGGCA
Core168	CCTGATTACTACGTGAACCATCACCCAAATCACCCTAAAG
Core169	TTGAATGGCCCTTCTGACCTGAAAGCCAACAGAGATAGAATCACCAGT
Core170	CGTTCTAGCTGTTTATATATCCCATCCCGGTC

Table S5. DNA sequences of the funnel-shaped DNA origami (5).

Name	Sequence
Core171	TTTTTGTTTAAAGTACTTTCGAGCCAGTAATA
Core173	TTCGGGAAACGCAAAGTGCTTTCG
Core174	AGAACAAGCAAGCTTGAGTTGATTGGTCAATAACCTGTTT
Core175	TTTTAGTTAATCCAATCGCAAGACTGTAAATGTGGCGAAAAACGCCAG
Core176	CCAACCTATAATATCACAAAGTCAGAGGGTAA
Core177	CGTCGCTATTAATTTTAATTCGAGGCTTAGAGCTTAATCAATATATGT
Core178	GCCCTTCACTGAGAGAGCGAATTAACCAAGTT

Table S6. DNA sequences of the funnel-shaped DNA origami with ssDNA overhangs for attachment of complementary modified ssDNA strands and cholesterol-tagged sequences.

Name	Sequence
Core14_O1	TTCCTTCTATGCATCTTTTTTGGAAGTTTCATTCCAACTAAAGTACGGT
Core36_O1	TTCCTTCTATGCATCTTCGTCACCAGCAGCCCTCACTAACGGCATAGTAA
Core40_O1	TTCCTTCTATGCATCTTACACTATCATAACCCTC
Core57_O1	TTCCTTCTATGCATCTTTTTAGTACCTTTAATTGAACAGGTCAGGATTA
Core77_O1	TTCCTTCTATGCATCTTTTTGAACAACTAAAGGACGGAGTGACACCGA CTAGACGTTA
Core94_O1	TTCCTTCTATGCATCTTTTTAAAAGGCTCCAAAACGTTGAAA
Core119_O1	TTCCTTCTATGCATCTTCTGTATGGGATTTTGCTGTTTAGACTGGATAGC
Core172_O1	TTCCTTCTATGCATCTTTTTTTTTCGCCCACGCAAAGGTGGCGCAATAAT
Core179_O1	TTCCTTCTATGCATCTTTTTAAAGCGGATTGCATACTATTATAGTCAGA
Core11_O1	GTAGCAACGAATTGAGTTTTTTTTTTTCAGCATGCTAGCTAG
Core28_O1	CTTCCACCACCCTCATACGGTCAATGACCTTCATTTTTTTTTTCAGCAT GCTAGCTAG
Core41_O1	TGAGAGATGACAGCATCGGTTTTTTTTCAGCATGCTAGCTAG
Core43_O1	CCACCCTCGCGAAACAGGAACGAGGTTTTTTTTTTCAGCATGCTAGCTAG
Core90_O1	AGGTGGCACAATAAAGCCTCAGAGCATTTTTTTTTTCAGCATGCTAGCTAG
Core93_O1	AGAAAAGCATTAAACGGTTTTTTTTTTCAGCATGCTAGCTAG
Core108_O1	AAATACGTAACGATTATACTTTTTTTTTTCAGCATGCTAGCTAG
Core124_O1	TAACACTGGGGCTTGACGTTAATAATTCAGCATGCTAGCTAG
Core135_O1	GCTGAGGCAGGTAAAGTTAATGCCGGAGAGGGTAGTTTTTTTTCAGCA TGCTAGCTAG
Core162_O1	AATCGGTTCAATGACAACATTTTTTTTCAGCATGCTAGCTAG
3'CholSequ.	GATGCATAGAAGGAA/3CholTEG/
5'CholSequ.	/5CholTEG/CTAGCTAGCATGCTG

2. Structural characterization of the DNA origami porin

2.1 Agarose gel electrophoresis

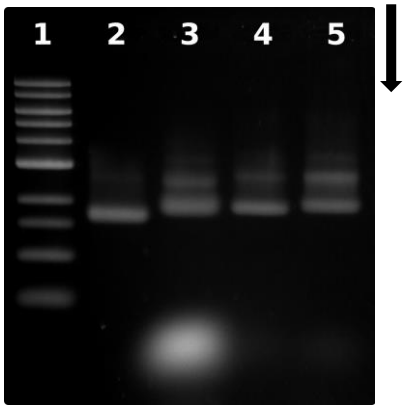

Figure S5. 1% agarose gel electrophoresis of the DNA origami porin in 11 mM $MgCl_2$ buffered to pH 8.3 with 45 mM Tris-borate, 1 mM EDTA. Bands were stained with GelRed (Cambridge Bioscience) and visualized using UV-transilluminaton. The arrow indicates the direction of migration in the gel.
Lane 1: 1 kbp DNA ladder (New England Biolabs).
Lane 2: 7249 base long M13mp18 single-stranded DNA scaffold (New England Biolabs).
Lane 3: Assembled DNA origami porin before purification from access staples in 40 mM Tris-HCl, 45 mM boric acid, 1 mM EDTA, 14 mM MgCl2, pH 8.2. The origami migrates marginally slower than the M13mp18 scaffold. The weaker lower band is likely to correspond to dimer formation.
Lane 4: Assembled DNA origami porin after purification by spin filtration with 100 kDa MWCO (Amicon) in 40 mM Tris-HCl, 45 mM boric acid, 1 mM EDTA, 14 mM MgCl2, pH 8.2. Spin filtration proofs to be an adequate method of purification from excess staples.
Lane 5: Sample from Lane 4 after 20 h incubation in the measurement buffer (1 M KCl, 10 mM MES, pH 6.0) at room temperature.

2.2 Note S1: Analysis of AFM imaging

After an accurate flattening procedure of the AFM images, we manually selected the profile sections across some clearly recognizable funnel-shaped DNA origami. An example of data analysis is presented in Figure S6A and S6B. For each origami we could determine 6 different typical lengths as indicated in Figure S6C. The section profile are shown in Figure S6B with the values measured for the different segments of the funnel DNA origami (see Figure S6C). The total number of origami analysed is 10 and the resulting data is presented in Table S7. The error is the standard deviation of the measurement and accounts for structural differences between different origami.

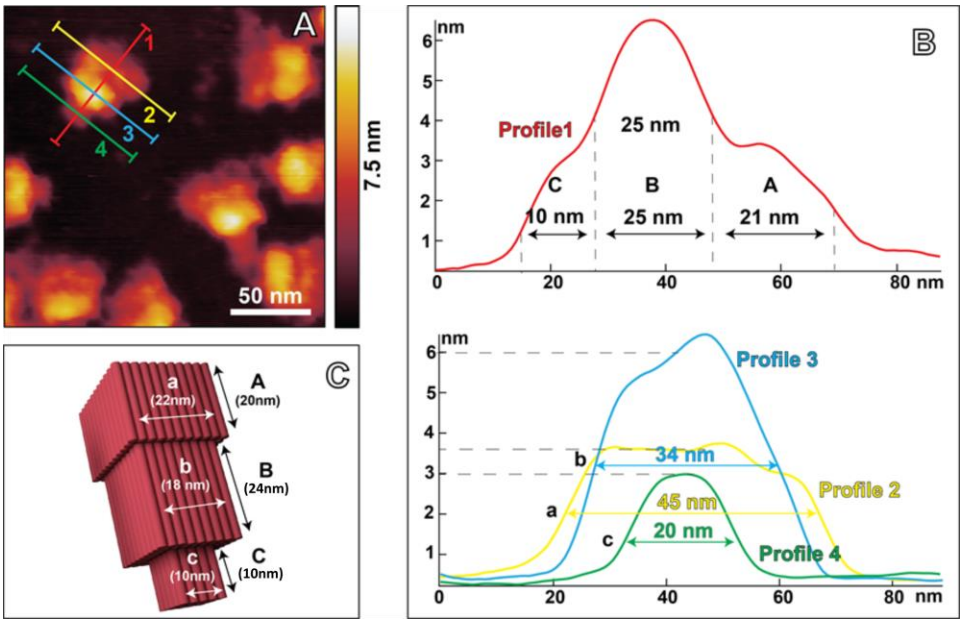

Figure S6: Illustration of the data analysis process to determine the dimensions of the DNA origami porin via AFM imaging. A) AFM image of the DNA origami porin. Cross-sections 1-4 indicate the evaluated dimensions. Generally, isolated and shape-preserved structures were preferred for the analysis. The profiles (B) were used to extract the dimensions of the different segments of the origami. The schematic representation of designed funnel is presented in C) with the letters (A, B, C and a, b, c) used to denominate the segments. Expected dimensions of the origami design are indicated, assuming an anhydrated helix diameter of 2 nm. The results of the analysis are presented in Table S7.

As a general remark, the values presented are the dimensions of "dry" DNA origami collapsed on the mica surface imaged with a finite-sized AFM tip (9±2 nm of nominal radius). Consequently, even if directly related, they only partially reflect the actual dimensions of hydrated DNA origami in solution. The purpose of the AFM investigation was to ensure accurate folding, not to obtain precise and quantitative information on the actual dimensions of the structures. It should also be noted that the imaging was performed before the addition of cholesterol staples, since the required access does not allow for the imaging with a clean background.

Table S7: Dimensions of the different segments of the funnel-shaped DNA origami porin. The letters denominate the segments as indicated in Figure S6C. The error is the standard deviation of the measurements and reflects the structural differences of 10 selected DNA structures.

	A	B	C	a	b	c
Value (nm)	20.8±2.5	23.6±2.1	11.0±1.7	46.7±2.0	35.8±2.0	18.9±2.0

The analysis of the height distribution of the DNA origami deposited on the mica surface is presented in Figure S7. A histogram is obtained from the height distribution in the AFM image (Figure S7A), in which the most recurrent protruding heights of the sample appear as peaks of the distribution. Up to 5 Gaussian peaks are necessary to properly describe the height distribution. The first peak (Peak 0 in Figure S7A and Table S8) corresponds to the mica surface. Peak 1 (≈ 0.2 nm protruding from the mica surface) and Peak 2 (≈ 0.9 nm protruding from the mica surface) are attributed respectively to small contaminations on the surface and partially unfolded structures. Finally, Peak 3 (≈ 2.67 nm protruding from the mica surface) and Peak 4 (≈ 4.95 nm protruding from the mica surface) are attributed respectively to two DNA layers (segment A and C of Figure S6C) and four DNA layers (segment B of Figure S6C). This is corroborated by the roughly double value of the protruding features and of the "Height" parameters of the peaks. The values of the FWHM of the Peak 3 and 4 are symptom of a big variability of the final conformation of the "dry" origami on the mica surface.

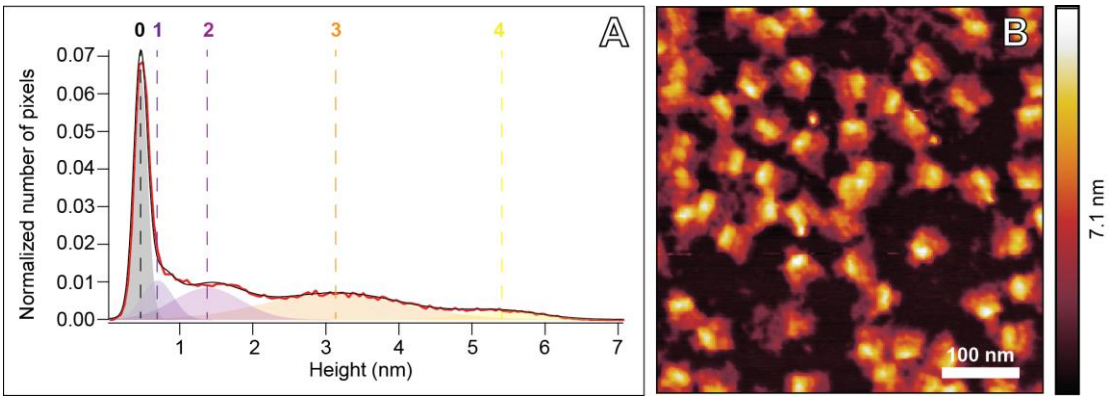

Figure S7. A) Histogram of height distributions obtained from the AFM image in (B). The histogram of the height can be fitted using 5 Gaussians. The resulting parameters of the fit are presented in Table S8. The image was acquired in air in Amplitude Modulation mode and flattened using standard AFM software. The structures look collapsed on the mica surface with the central segment, composed of 4 double strands DNA layers on top of each other, clearly higher than the other 2 segments (only two double strands DNA layers). Although the funnel-shape is clearly recognizable most of the structures are deformed because of the "dry" imaging condition.

Table S8. Results of the multi-peak fitting of the histogram (Figure S7A) obtained from the AFM image (Figure S7B). The "Location" parameter represents the x-position of the Gaussian center. The "FWHM" is the Full-Width-Half-Maximum of the Gaussian and the "Height" reflects the intensity of the peak.

	Peak 0	**Peak 1**	**Peak 2**	**Peak 3**	**Peak 4**
Location (nm)	0.463	0.695	1.38	3.13	5.41
FWHM (nm)	0.219	0.490	1.09	2.28	1.28
Height	0.0647	0.0104	0.0084	0.0071	0.0022

3. Experimental ionic current recordings

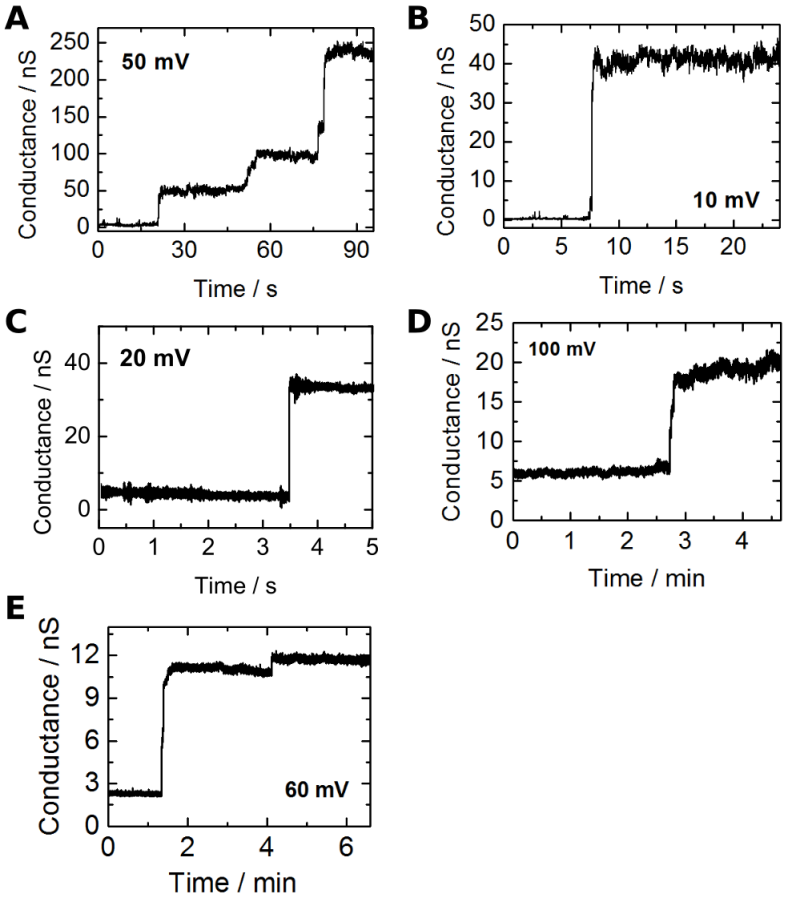

Figure S8. Additional ionic current traces recorded in the presence of the DNA origami porin at 1 kHz sampling rate in 1 M KCl, 10 mM MES, pH 6.0. Stepwise increase in conductance is attributed to the insertion of one or more DNA origami porins.

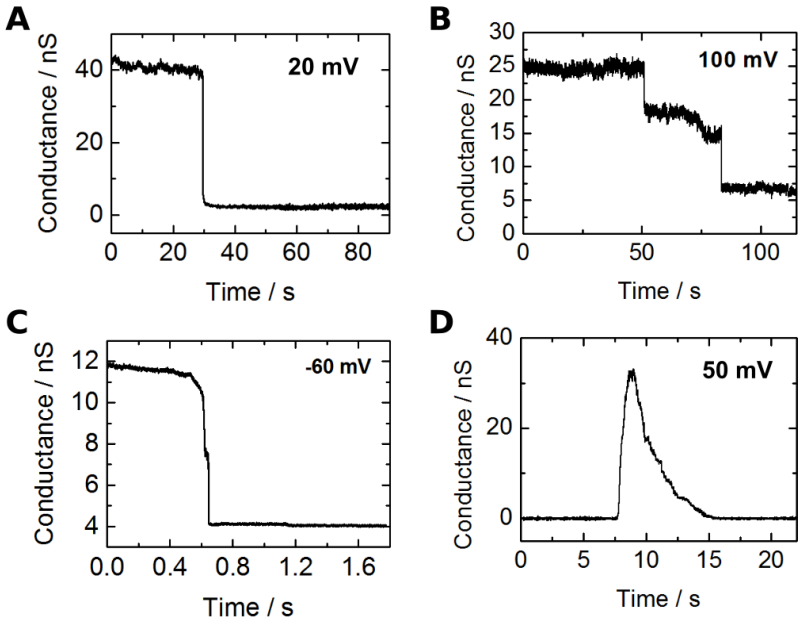

Figure S9. Additional ionic current traces recorded in the presence of the DNA origami porin at 1 kHz sampling rate in 1 M KCl, 10 mM MES, pH 6.0. A) – C) Closure steps. The stepwise reduction in ionic conductance could be caused by pores flipping out of the membrane. Closures were often observed during an I-V recording after changing the voltage. D) Events with this characteristic shape but variable conductance were regularly observed in the presence of the DNA origami porin. They could be caused by unsuccessful insertion attempts.

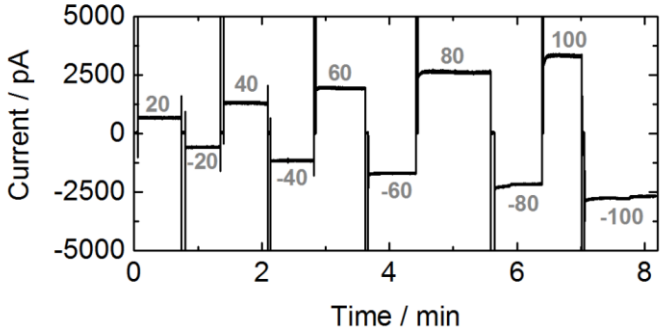

Figure S10. Example I-V trace of a stable, lower-noise DNA porin with a conductance of approximately 30 nS, recorded at 1 kHz. The DNA porin remained inserted for the entire IV-recording and did not "close" at higher voltages as shown in Figure S9. All IV-curves were recorded after a clear insertion step was observed.

4. Molecular dynamics simulations

4.1 Arrangement of lipid head groups at lipid-DNA interface

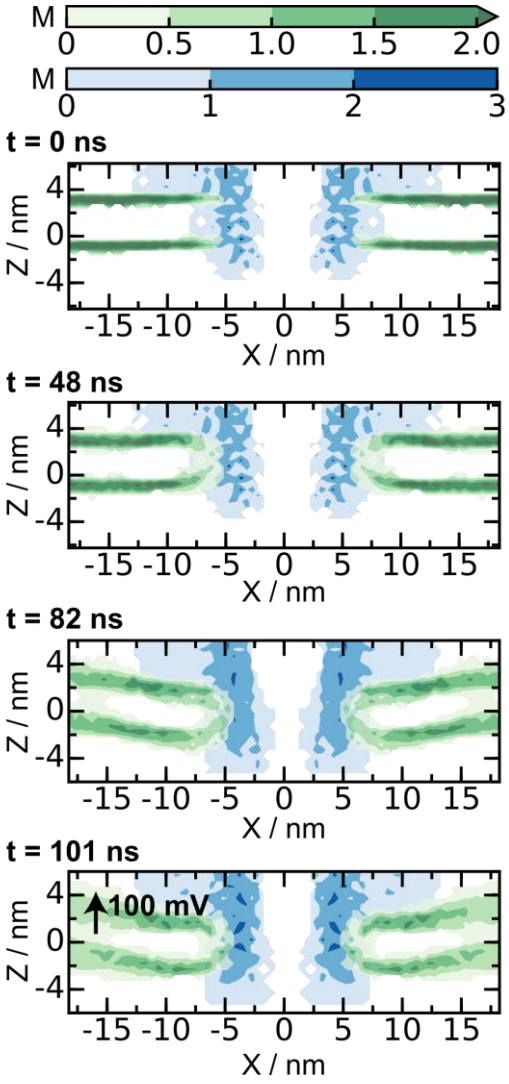

Figure S11. Local density of lipid head groups (phosphorus atoms, green) and DNA (phosphorus atoms, blue) near the lipid-DNA porin interface at several stages of the MD simulation. From top to bottom, the snapshots illustrate the state of the system prior to the equilibration simulation (0 ns), at the end of the equilibration simulation performed having all non-hydrogen atoms of the DNA origami porin restrained to their initial coordinates (48 ns), at the end of the unrestrained equilibration simulation (82 ns), and at the end of the simulation performed under +100 mV transmembrane bias (101 ns). In the last panel, the black arrow indicates the direction of the transmembrane bias. Each snapshot was computed by averaging the coordinates of the phosphorus atoms over a short (1 ns) fragment of the 48-ps sampled trajectory nearest to the point of interest. To increase accuracy, the density maps were radially averaged about the z-axis (which is also the symmetry axis of the DNA origami porin).

4.2 Local concentration of ions near DNA origami porin

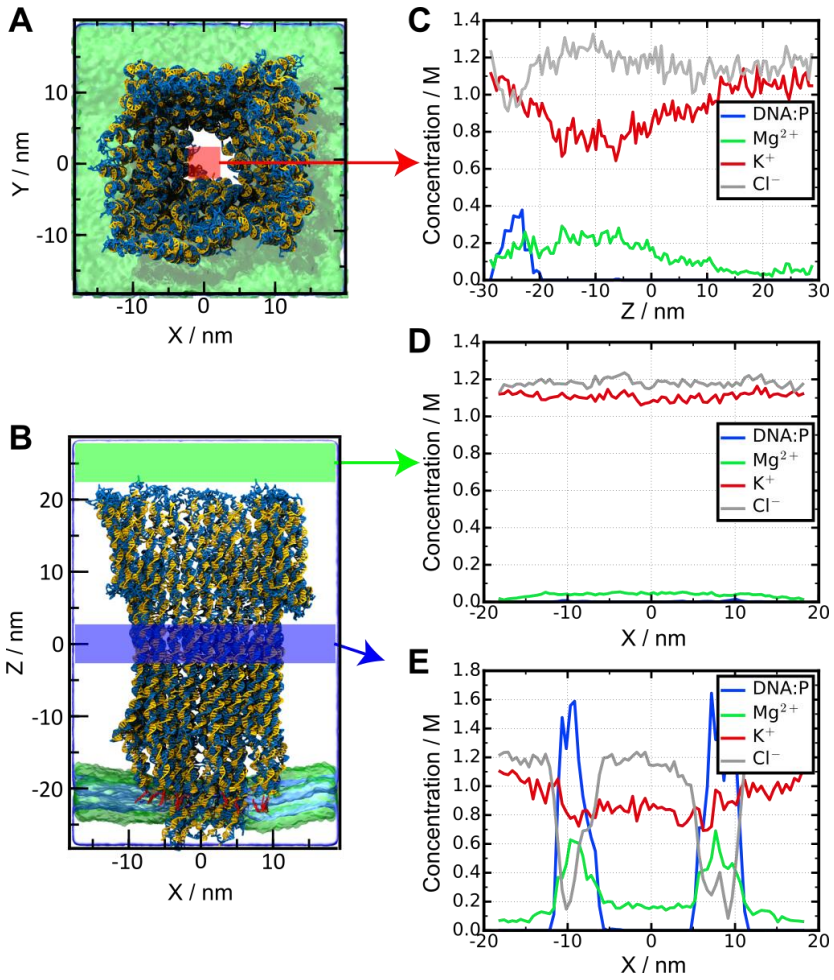

Figure S12. Local concentration of ions in MD simulation of the DNA origami porin. A, B) All-atom model of the DNA porin (blue and yellow) embedded in a lipid membrane (green) at the end of the equilibration simulation. Cholesterol tags are shown in red. C) The local concentration of ions and DNA phosphate atoms along the symmetry axis of the DNA origami porin (the Z axis). The ion and DNA phosphate concentrations were averaged over the [-2 nm < X < 2 nm, -2 nm < Y < 2 nm] section of the system (highlighted in red in panel A) and over the 19.2 ns unrestrained equilibration trajectory sampled every 240 ps. D,E) The local concentration of ions and DNA phosphate atoms at the two XY cross sections of the simulated system, which are highlighted in green and blue in panel B. Data shown in panels D and E were averaged over the entire range of Y value and over [-2.5 nm < Y < 2.5 nm], respectively, and over the 19.2 ns unrestrained equilibration trajectory sampled every 240 ps.

4.3 Histograms of simulated ionic current

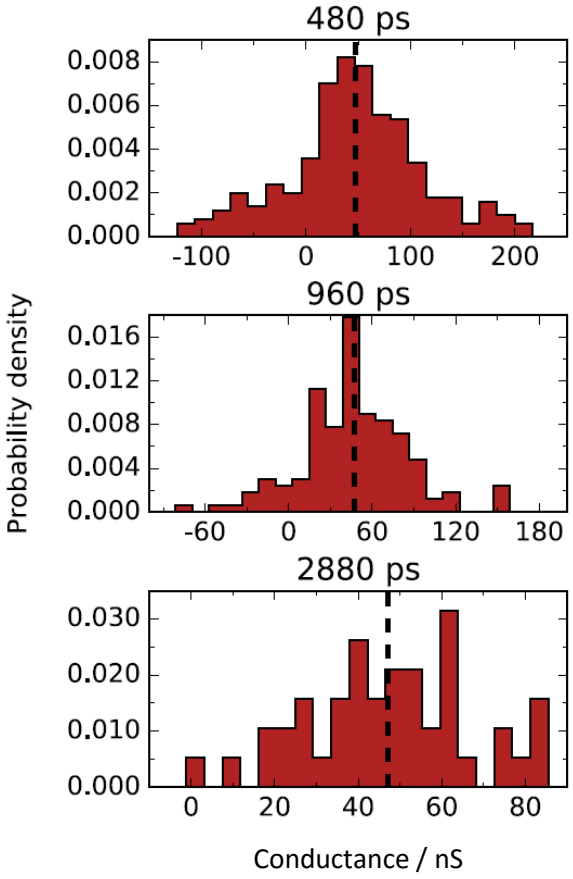

Figure S13. Normalized histograms of ionic conductance in MD simulations of the DNA origami porin. The conductance histograms were obtained by splitting the ionic current traces at +100 mV, +30 mV, -30 mV and -100 mV into blocks of specified duration, averaging the currents within each block, dividing the average current in each block by the transmembrane bias and concatenating the resulting conductance values into one data set. In each column, the histograms differ by the size of the blocks the currents were averaged over; the block size is specified at the top of each graph. The dashed lines indicate the mean conductance values. Note the difference in the scale of the horizontal axes.

4.4 Note S2: Caption for Movie S1

Molecular dynamics simulation of DNA origami porin in a lipid bilayer membrane. The DNA strands are shown in blue and yellow; the cholesterol groups are shown in gray. The lipid bilayer membrane is drawn as a green molecular surface. The slide bar at the lower right corner indicates the progression of the trajectory in nanoseconds (ns). The first 32 ns illustrate the equilibration trajectory, which is followed by a simulation at a +100 mV bias. At the beginning of the movie, a static rendering of the system is rotated to show the overall structure. The second stage of the movie illustrates the structural fluctuations during the equilibration; lipid molecules facing the viewer are hidden for clarity. In the last stage of the movie, the half of the DNA origami porin facing the viewer is removed and the transmembrane region of the channel is enlarged to illustrate the ion transport. Red spheres show instantaneous locations of potassium ions. For clarity, only those potassium ions that contribute significantly to the transmembrane ionic current (about 10% of all ions) are shown.